ISSN 1070-3632, Russian Journal of General Chemistry, 2014, Vol. 84, No. 9, pp. 1793–1798. © Pleiades Publishing, Ltd., 2014.
Original Russian Text © S.N. Eliseeva, E.G. Tolstopyatova, T.A. Babkova, V.V. Kondratiev, 2014, published in Zhurnal Obshchei Khimii, 2014, Vol. 84, No. 9, pp. 1557–1562.

Nanocomposite Electrode Materials Based on Poly(3,4-Ethylenedioxythiophene) with Incorporated Gold and Palladium: Preparation and Morphology Study

S. N. Eliseeva, E. G. Tolstopyatova, T. A. Babkova, and V. V. Kondratiev

St. Petersburg State University, Universitetskii pr. 26, St. Petersburg, 198504 Russia
e-mail: vkondratiev@mail.ru

Received April 7, 2014

Abstract—Chemical deposition of ultrafine gold and palladium particles into poly(3,4-ethylenedioxythiophene) matrix has yielded the metal-containing polymer composites. Their structure has been studied as affected by duration of reduced polymer immersion into the metal salts solution, and by concentration of the latter. Morphology features of the composite films (size and concentration of metal particles) have been elucidated by scanning and transmission electron microscopy. The mixed clusters have been formed predominantly in the course of preparation of bimetal composite films via sequential deposition of gold and palladium; the isolated palladium clusters nucleate slower due to the gold–palladium alloys formation. Longer deposition of the metals leads to increase in the nanoparticles size and their concentration in the composite. Properties of the prepared materials have been demonstrated using the model electrochemical reactions.

Keywords: polymer composite, poly(3,4-ethylenedioxythiophene), metal nanoparticle, cyclic voltamperometry, electron microscopy

DOI: 10.1134/S1070363214090254

In recent years a new trend in development of electrode materials has emerged: modification of conductive polymers with nanosized particles of metals and their compounds. Such hybrid organic-inorganic materials are especially interesting due to the advantageous functional properties of the highly disperse nanostructured matter incorporated into the conductive matrix [1–7]. In general, such composites exhibit properties combining those typical of the conductive polymer constituting the matrix and those of the incorporated metal nanoparticles.

We have previously demonstrated [8–11] that redox interaction between the reduced form of poly(3,4-ethylenedioxythiophene) (PEDOT) and ions of electropositive metals (palladium or gold) can be applied to produce metal nanoparticles at the polymer surface and inside its pores. We have investigated electrochemical behavior of the PEDOT/Pd and PEDOT/Au composite films [8–10] and morphology of the PEDOT/Pd films [11]. Morphology of the PEDOT/Au films has not been studied in detail in the above-cited papers.

Here we report new data on morphology of the PEDOT/Au films and possibility of the Au–Pd mixed metal clusters formation. The bimetal Au–Pd particles are extremely interesting: catalytic properties of the mixed particles have been demonstrated to be enhanced as compared to those of the corresponding individual particles [12–15]. For example, thin palladium films on gold support are more active towards oxygen reduction than pure palladium and gold [14, 15]; the effect is caused by the formation of Pd–Au alloys at the interface.

The composites prepared in this work are applicable in electroanalysis as micro- and nano-electrode assemblies, the incorporated metal particles acting as electrodes in the electrochemical process, and the conductive polymer behaves as the integrating conducting matrix. When metal nanoparticles are deposited onto the surface of carbon or metal electrodes, the former are agglomerated to form larger structures, whereas the polymer matrix can stabilize the nano-particles to prevent the aggregation. This approach is suitable to produce the catalysts based on

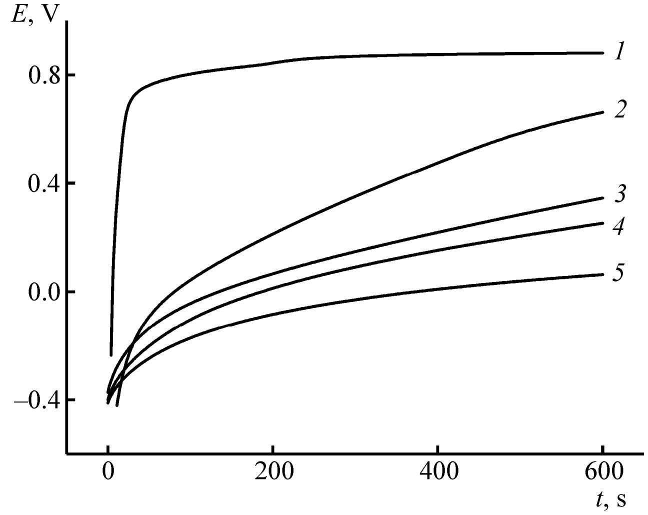

Fig. 1. Potential of PEDOT film as a function of duration of its immersion in the $HAuCl_4$ solution. $HAuCl_4$ concentration, mol/L: (*1*) 5×10^{-3}, (*2*) 5×10^{-4}, (*3*) 2.5×10^{-4}, (*4*) 1.2×10^{-4}, and (*5*) 5×10^{-5}; $[H_2SO_4] = 0.1$ mol/L.

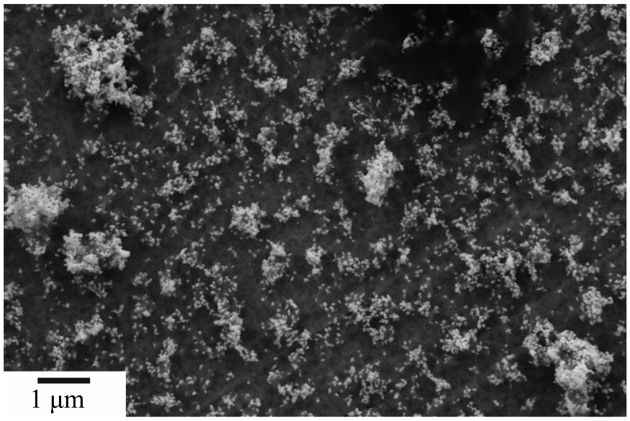

Fig. 2. Morphology of the PEDOT/Au film (scanning electron microscopy; 120 s deposition at 5×10^{-3} mol/L of $HAuCl_4$).

metals for future application in fuel cells and electrocatalytic transformation of organic compounds.

PEDOT/Au films. In order to incorporate metal gold into the electrochemically prepared PEDOT film, the latter was pre-reduced at –0.4 V in aqueous H_2SO_4 (0.1 mol/L) during 150 s, and then immersed into aqueous H_2SO_4 (0.1 mol/L) containing required concentration of the gold(III) complexes (5×10^{-4}–5×10^{-3} mol/L). The duration of gold deposition into the films was 30 and 400 s. When gold(III) ions (showing high redox potential $E = 1.002$ V [16]) came in contact with the reduced form of PEDOT film, the redox process occurred leading to the formation of metal gold particles and oxidation of the pre-reduced polymer groups.

$$3\mathrm{PEDOT}^0 + \mathrm{AuCl}_4^- + 3\mathrm{A}^- \rightarrow [(\mathrm{PEDOT}^+\mathrm{A}^-)_3\mathrm{Au}^0] + 4\mathrm{Cl}^-.$$

In the above equation, PEDOT stands for the polymer fragment participating in the redox process (four repeating units) and A^- designates the doping anions (anions of the electrolyte present in the solution during the synthesis). Noteworthily, the overall stability constant of the $AuCl_4^-$ complex is 5×10^{22} L/mol [17].

The stepwise stability constants corresponding to the chloride complex dissociation $AuCl_4^- \rightleftarrows AuCl_3 + Cl^-$ are of $10^{4.9}$ L/mol ($\mu = 0$) and $10^{5.02}$ L/mol (0.1 mol/L H_2SO_4) [18]. Hence, the dissociation degree of chloride complexes of gold(III) was extremely low, and their higher forms prevailed in the solution.

Evolution of potential of the PEDOT-modified glassy carbon electrode in the course of redox interaction with gold(III) is shown in Fig. 1. Even in the very first moments after the immersion in the $HAuCl_4$-containing solution the potential of the PEDOT film (pre-reduced at E = –0.4 V) was increasing due to the oxidation of the film accompanied with the formation of metal gold. The potential change was the fastest at the highest $HAuCl_4$ concentration used (5×10^{-3} mol/L), and initially rapidly growing potential became constant after 1–3 min. At lower concentrations of $HAuCl_4$ the potential growth was slower. The observed kinetic features could be explained by the change of the limiting factor in the course of the interaction. Initially the gold deposition rate was likely limited by the nucleation and stabilization of the formed gold clusters; in the later stages of the process the rate-limiting stage was gold ions diffusion to the growing particles in the solution as well as in the film.

Incorporation of metal gold in the PEDOT films was confirmed by the EDXRF analysis: the peaks at 1.5–2.5 keV were observed in the X-ray fluorescence spectra of the prepared composites, the emission energy corresponding to gold atoms.

According to the scanning electron microscopy data, the PEDOT/Au composite film prepared at high concentration of the gold complex (5×10^{-3} mol/L) contained ultradispersed gold particles forming the agglomerated clusters (Fig. 2). The isolated particles were of 100–200 nm, but most of them formed larger aggregates.

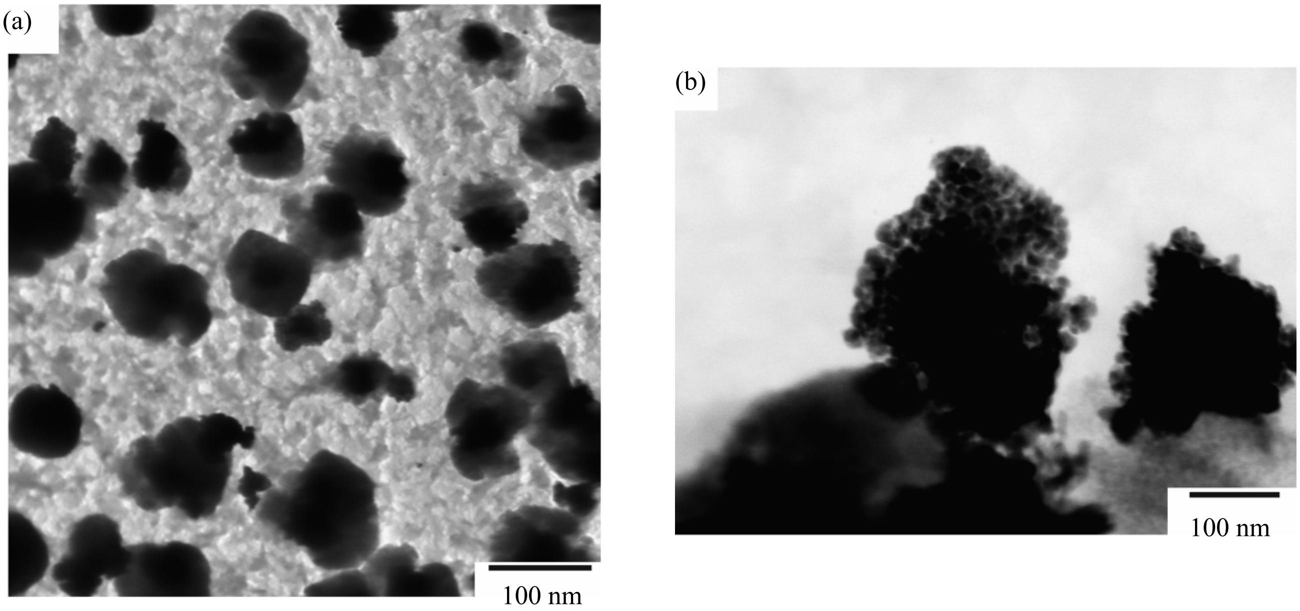

Fig. 3. Morphology of the PEDOT/Au film [transmission electron microscopy, 60 s (a) and 120 s (b) deposition at 5 × 10^{-3} mol/L of $HAuCl_4$].

Gold particles incorporated in the prepared composite were studied in detail by transmission electron microscopy. The 70–100 nm isolated gold particles were to be seen in the images (Fig. 3a); the particles were composed of smaller clusters (Fig 3b).

Transmission electron microscopy of the PEDOT/Au composite film prepared via the 60 s gold deposition from the less concentrated $HAuCl_4$ solution (5 × 10^{-4} mol/L) revealed the non-uniformly distributed Au nanoparticles sized from ~5 nm to 20–30 nm. Hence, the dilution of the starting $HAuCl_4$ solution decreased both the size and concentration of the gold particles formed at the electrode surface. Therefore, varying concentration of $HAuCl_4$ allowed to control the gold particles size and their density number in the composite.

PEDOT/Au/Pd bimetal composite films. We further investigated the possibility of the bimetal composites preparation (in particular, gold particles prepared at the PEDOT film were decorated with palladium particles) and studied the properties of the so formed PEDOT-based materials.

The PEDOT/Au/Pd composite films were prepared following the three-stage procedure: synthesis of PEDOT film at the electrode surface; reduction of the film and the electroless deposition of gold particles into the polymer (see above); and reduction of the PEDOT/Au composite and the electroless deposition of palladium particles from $PdCl_2$ solution. Similarly to the above-described case of gold deposition from $HAuCl_4$ solution, the contact of the reduced PEDOT/Au film with $PdCl_2$ solution was accompanied with spontaneous redox process of Pd(II) reduction to Pd(0) and partial oxidation of the polymer. The latter stage could be represented by the following scheme.

$$2\mathrm{PEDOT}^0/\mathrm{Au}^0 + \mathrm{Pd}^{2+} + 2\mathrm{A}^- \rightarrow (\mathrm{PEDOT}^+\mathrm{A}^-)_2\mathrm{Au}^0/\mathrm{Pd}^0.$$

In this equation, PEDOT stands for the polymer fragment participating in the redox process (four repeating units) and A^- designates the doping anions (sulfate or chloride ions, the latter coming from $PdCl_2$ solute).

Chemical deposition of palladium particles into the PEDOT and PEDOT/Au films was performed using $PdCl_2$ solutions (5 × 10^{-3} to 2.5 × 10^{-4} mol/L) containing 0.1 mol/L of H_2SO_4. Kinetics of the electroless potential change in the course of the process is illustrated by Fig. 4. From the plots it is seen that the potential growth has been significantly faster in the case of the PEDOT/Au composite as compared to the deposition involving the source PEDOT film. Moreover, in the case of the Au-containing composite the stationary potential was noticeably higher (PEDOT, E = 0.42 V; PEDOT/Au, E = 0.51 V). Both effects could be due to the decreased free energy of Pd

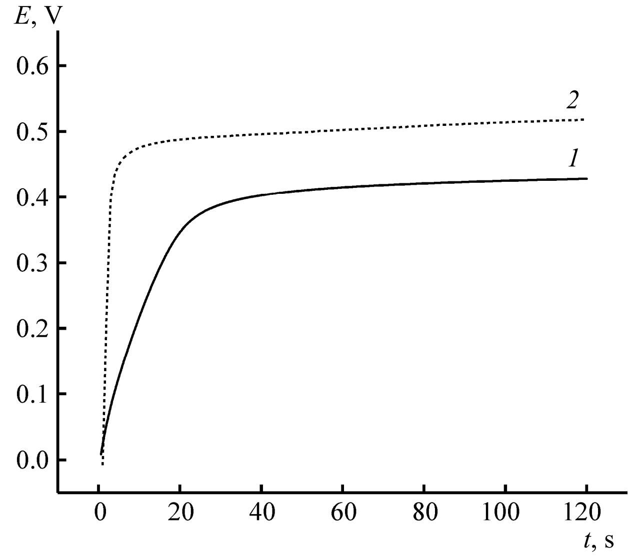

Fig. 4. Potentials of PEDOT film (*1*) and of PEDOT/Au composite film (*2*) as a function of duration of their immersion in the $PdCl_2$ solution. $[PdCl_2] = 5 \times 10^{-3}$ mol/L, $[H_2SO_4] = 0.1$ mol/L.

crystals nucleation at Au particles caused by the formation of the metals alloy. Hence, palladium nucleation should initially occur predominantly at the gold particles incorporated in the film.

The deposition of the metal palladium into the PEDOT/Au films was confirmed by EDXRF analysis: the strong peaks with the emission energy corresponding to both gold and palladium atoms were observed in the X-ray fluorescence spectra. The ratio of the peaks intensity depended on the deposition time, and was non-uniform along the sample surface.

Comparison of transmission electron microscopy images showing morphology of the initial PEDOT/Au films and that of the derived PEDOT/Au/Pd bimetal composites (Fig. 5) revealed that the film immersion into the solution of palladium salt resulted in the formation of 20–30 nm Pd particles at the unoccupied polymer surface. Further immersion of the film into $PdCl_2$ solution increased the formed particles concentration. The Pd particles formed at the surface of larger (100–200 nm) gold particles could not be distinguished by transmission electron microscopy due to the comparable density of the metals.

The nucleation of palladium at the gold particles contained within the PEDOT/Au films was indirectly confirmed by the faster palladium loading into the PEDOT/Au film as compared to the case of the untreated PEDOT film. Initially, palladium was evidently deposited at the gold particles; later, palladium could be deposited at the unoccupied polymer areas. That was demonstrated by the cyclic voltammetry results discussed below.

Electrochemical properties of the prepared structured composite electrodes were illustrated using the model reactions occurring exclusively in the presence of the corresponding metals: the formation of gold and palladium oxides at the PEDOT/Au and PEDOT/Au/Pd surface upon the films oxidation in the electrolyte solutions.

In particular, more drastic increase of the anodic current at more positive potentials (gold oxidation) was observed in the cyclic voltammograms of the PEDOT/Au films and of the polycrystalline gold electrode (Fig. 6); cathodic peak of Au_2O_3 reduction appeared at $E = 0.9$ V.

$$2Au + 3H_2O \rightleftarrows Au_2O_3 + 6H^+ + e^-.$$

Cyclic voltammograms of the PEDOT/Au/Pd films are shown in Fig. 7. Curve *1* contains only the peak of

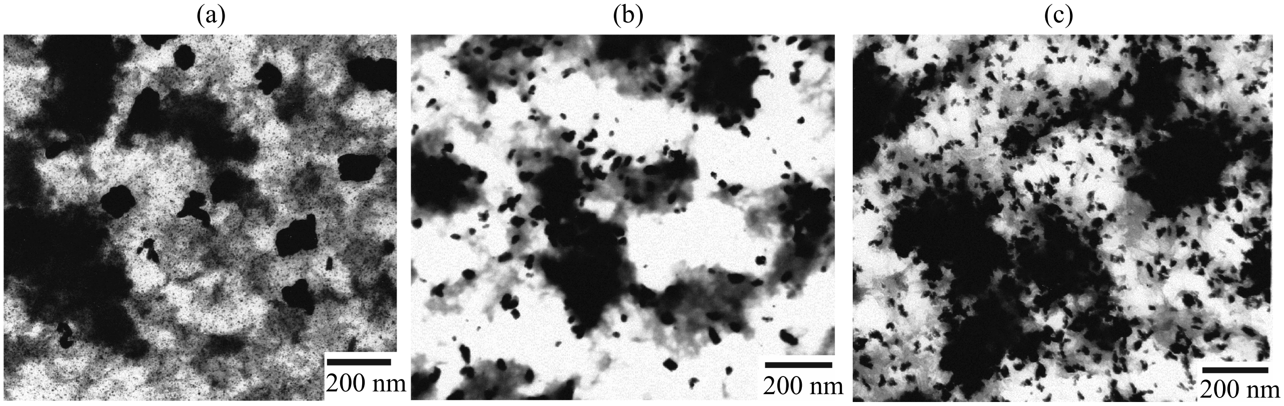

Fig. 5. Transmission electron microscopy images of the PEDOT/Au (deposition time 120 s) (a) and the PEDOT/Au/Pd [gold deposition time 120 s; palladium deposition during 30 s (b) and 120 s (c) at 2.5×10^{-3} mol/L of $PdCl_2$] films.

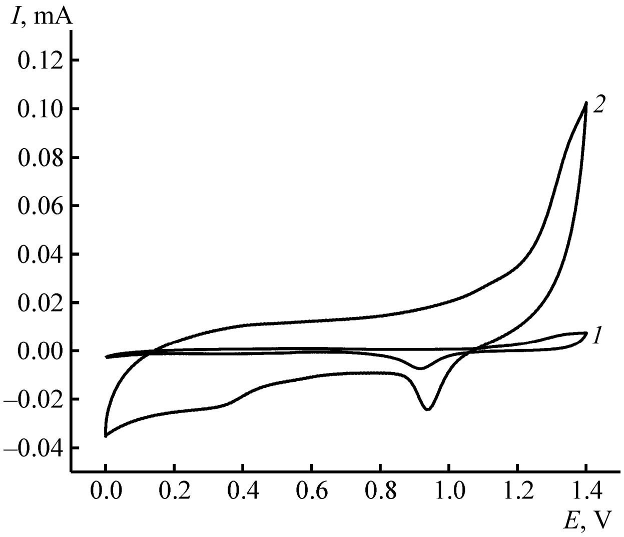

Fig. 6. Cyclic voltammograms (0.1 mol/L $HClO_4$) of polycrys-talline gold electrode ($S = 0.07$ cm^2) (*1*) and of PEDOT/Au composite at the electrode of equal area (gold deposition during 400 s at 3×10^{-3} mol/L of $HAuCl_4$) (*2*).

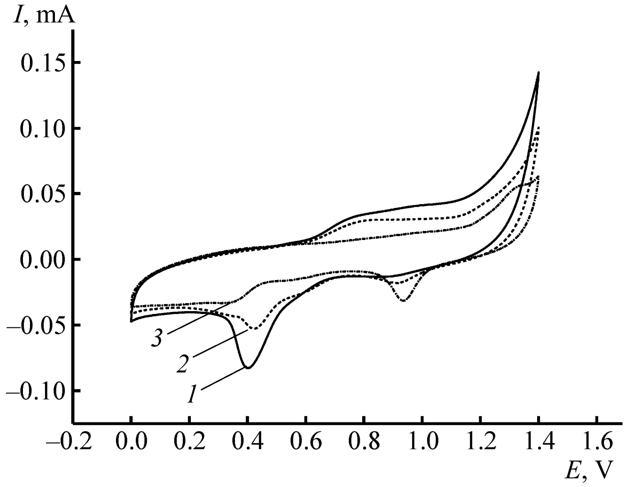

Fig. 7. Cyclic voltammograms (0.1 mol/L $HClO_4$) of the PEDOT/Au/Pd composite (gold deposition during 400 s from 3 mmol/L solution of $HAuCl_4$; palladium deposition during 120 s from 5 mmol/L solution of $PdCl_2$): 3 cycle (*1*), 18 cycle (*2*), and 33 cycle (*3*).

palladium oxide reduction, whereas the peak of gold oxide reduction was absent (cf. Fig. 6, curve *2*). This confirmed that the deposited palladium completely covered the gold particles. The prolonged cyclic treatment of the PEDOT/Au/Pd film led to appearance and strengthening of the gold oxide reduction peak, and the palladium oxide reduction peak simultaneously disappeared (Fig. 7, curves *2* and *3*). Evidently, the gradual change of the curve shape was due to palladium dissolution from the gold particles surface. Noteworthily, palladium dissolution was not observed in the case of the PEDOT/Pd film (cyclic treatment at up to +1 V, other conditions being the same).

To conclude, the collected data demonstrated the possibility of formation of nanocomposite metal-polymer structures upon spontaneous reduction of gold and palladium ions at the conductive polymer film. The amount of the deposited metals increased regularly with longer deposition; the increase in $HAuCl_4$ concentration yielded larger gold particles. The gold particles contained in the PEDOT/Au/Pd composite were completely covered with metal palladium; however, the palladium shell was irreversibly dissolved in the course of prolonged cyclic electrochemical treatment of the film.

EXPERIMENTAL

The following chemicals were used: 3,4-ethylenedioxythiophene (Aldrich), anhydrous lithium perchlorate (“chemically pure” grade, calcined in the oven to constant mass), acetonitrile (“specially pure” grade, Cryochrom, 0.008 wt% of water), gold(III) chloride (10 g/L solution, Tekhnoanalit), palladium(II) chloride (99%, Aldrich), sulfuric acid (“chemically pure” grade), perchloric acid (“chemically pure” grade), and distilled water. $AuCl_3$ solutions were prepared by dilution of the stock solution with aqueous sulfuric acid (0.1 mol/L). $PdCl_2$ solutions were prepared by dissolving $PdCl_2$ powder in aqueous sulfuric acid (0.1 mol/L).

Electrochemical preparation of PEDOT films was performed at the glassy carbon electrode ($S = 0.07$ cm^2) under galvanostatic conditions at the current density of 1 mA/cm^2; the modifying solution contained 0.05 mol/L of 3,4-ethylebedioxythiophene and 0.1 mol/L of $LiClO_4$ in acetonitrile.

Electrochemical measurements were carried out using the glass three-electrode cell. The measured potentials were reported as referenced to the silver chloride electrode in saturated NaCl solution.

Electrochemical synthesis and voltammetric characterization were performed using the AUTOLAB PGSTAT-30 instrument (ECO CHEMIE, the Netherlands).

Scanning electron microscopy studies of the surface morphology were performed using the Zeiss SUPRA 40VP scanning electron microscope (Carl Zeiss, Germany) in the secondary electron beam at the accelerating voltage of 15 kV, at high vacuum in the chamber. Elemental composition of the films was determined by X-ray fluorescence microanalysis using the Oxford Instruments X-act energy-dispersing spectrometer. The specimens were prepared at platinum-spattered quartz crystals.

Transmission electron microscopy studies were performed using the LIBRA 200 FE (Carl Zeiss, Germany) and Philips CM10 TEM (Philips, the Netherlands) microscopes; the specimens were prepared via transfer onto the copper mesh.

ACKNOWLEDGMENTS

The experiments were carried out using the equipment installed in the "Physical methods of surface study" and "Nanotechnologies" Resource Centers of St. Petersburg State University.

This work was financially supported by the Russian Foundation for Basic Research (project no. 13-03-00984).

REFERENCES

1. Moutet, J.C., Ouennoughi, Y., Ourari, A., and Hamar-Thibault, S., *Electrochim. Acta*, 1995, vol. 40, p. 1827.
2. Podlovchenko, B.I. and Andreev, V.N., *Russ. Chem. Rev.*, 2002, vol. 71, p. 837. DOI: 10.1070/RC2002v071n10 ABEH000672.
3. Sih, B.C. and Wolf, M.O., *Chem. Commun.*, 2005, vol. 27, p. 3375. DOI: 10.1039/B501448D.
4. Frydrychewicz, A., Vassiliev, S.Yu., Tsirlina, G.A., and Jackowska, K., *Electrochim. Acta*, 2005, vol. 50, p. 1885. DOI: 10.1016/j.electacta.2004.08.041.
5. Ilieva, M., Tsakova, V., and Erfurth, W., *Electrochim. Acta*, 2006, vol. 52, p. 816. DOI: 10.1016/j.electacta.2006.06.015.
6. Terzi, F., Zanardi, C., Martina, V., Pigani, L., and Seeber, R., *J. Electroanal. Chem.*, 2008, vols. 619–620, p. 75. DOI: 10.1016/j.jelechem.2008.03.009.
7. Hatchett, D.W., Josowicz, M., Janata, J., and Baer, D.R., *Chem. Mater.*, 1999, vol. 11, p. 2989. DOI: 10.1021/cm990365m.
8. Eliseeva, S.N., Malev, V.V., and Kondrat'ev, V.V., *Russ. J. Electrochem.*, 2009, vol. 45, p. 1045. DOI: 10.1134/S1023193509090109.
9. Kondratiev, V.V., Babkova, T.A., and Eliseeva, S.N., *Russ. J. Electrochem.*, 2012, vol. 48, p. 205. DOI: 10.1134/S1023193512020061.
10. Pogulyaichenko, N.A., Hui So, Malev, V.V., and Kondratiev, V.V., *Russ. J. Electrochem.*, 2009, vol. 45, p. 1176. DOI: 10.1134/S1023193509100103.
11. Eliseeva, S.N., Ubyivovk, E.V., Bondarenko, A.S., Vyvenko, O.F., and Kondratiev, V.V., *Russ. J. Gen. Chem.*, 2010, vol. 80, no. 6, p. 1143. DOI: 10.1134/S1070363210060174.
12. Bukhtiyarov, V.I. and Slin'ko, M.G., *Russ. Chem. Rev.*, 2001, vol. 70, p. 147. DOI: 10.1070/RC2001v070n02ABEH 000637.
13. Gao, F. and Goodman, D.W., *Chem. Soc. Rev.*, 2012, vol. 41, p. 8009. DOI: 10.1039/C2CS35160A.
14. Ding, Y., Fan, F., Tian, Z., and Wang, Z.L., *J. Am. Chem. Soc.*, 2010, vol. 132, p. 12480. DOI: 10.1021/ja105614q.
15. Chen, M., Kumar, D., Yi, C.-W., and Goodman, D.W., *Science*, 2005, vol. 310, p. 291. DOI: 10.1126/science.1115800.
16. Panda, B.R. and Chattopadhyay, A., *J. Colloid Interface Sci.*, 2007, vol. 316, p. 962. DOI: 10.1016/j.jcis.2007.08.033.
17. Yatsimirskii, K.B. and Vasil'ev, V.P., *Konstanty nestoikosti kompleksnykh soedinenii* (Instability Constants of Complex Compounds), Moscow: Akad. Nauk SSSR, 1959.
18. Bekker, P.V.Z. and Robb, W., *Inorg. Nuclear Chem. Lett.*, 1972, vol. 8, p. 849. DOI: 10.1016/0020-1650(72)80234-4.